Materials Science and Engineering A 528 (2011) 3799–3808

Contents lists available at ScienceDirect

Materials Science and Engineering A

journal homepage: www.elsevier.com/locate/msea

Molecular-level simulations of shock generation and propagation in polyurea

M. Grujicic[a,*], B. Pandurangan[a], W.C. Bell[a], B.A. Cheeseman[b], C.-F. Yen[b], C.L. Randow[b]

[a] Department of Mechanical Engineering, Clemson University, Clemson, SC 29634, United States
[b] Army Research Laboratory – Weapons & Materials Research Directorate, Aberdeen, Proving Ground, MD 21005-5069, United States

ARTICLE INFO

Article history:
Received 5 January 2011
Received in revised form 18 January 2011
Accepted 19 January 2011
Available online 26 January 2011

Keywords:
Polyurea
Shock-wave generation and propagation
Molecular-level calculations

ABSTRACT

A non-equilibrium molecular dynamics method is employed in order to study various phenomena accompanying the generation and propagation of shock waves in polyurea (a micro-phase segregated elastomer). Several recent studies reported in the literature suggested that polyurea has a relatively high potential for mitigation of the effects associated with blast and ballistic impact. This behavior of polyurea is believed to be closely related to its micro-phase segregated microstructure (consisting of the so-called "hard domains" and a soft matrix) and to different phenomena/processes (e.g. inelastic-deformation and energy-dissipation) taking place at, or in the vicinity of, the shock front. The findings obtained in the present analysis are used to help elucidate the molecular-level character of these phenomena/processes. In addition, the analysis yielded the shock Hugoniot (i.e. a set of axial stress vs. density/specific-volume vs. internal energy vs. particle velocity vs. temperature vs. shock speed) material states obtained in polyurea after the passage of a shock wave. The availability of a shock Hugoniot is critical for construction of a high deformation-rate, large-strain, high pressure material models which can be used within a continuum-level computational analysis to capture the response of a polyurea-based macroscopic structure (e.g. blast-protection helmet suspension pads) to blast/ballistic impact loading.

1. Introduction

Due to the use of effective body armor, timely and effective evacuation, and efficient and advanced wound care, military personnel can today survive (previously fatal) injuries caused by blasts and bullets/fragments. However, even in the absence of their visible external injuries, the military personnel are often found to suffer from traumatic brain injury (TBI) after exposure to blast/shock waves/loads. Due to its resulting high direct and indirect economic costs to society at large (through lost earning potential of the affected and the burden of care imposed on their families), TBI has become an important societal problem. This has led to an urgent need for the development of novel head protection strategies requiring in-depth understanding of relationships between the morphology/structure (at different length scales) of the constituent materials and the activation/effectiveness of different blast-energy dissipation/dispersion mechanisms [1]. Once such knowledge is gained, new material systems with superior blast-energy dissipation/dispersion capabilities can be designed, synthesized, and their high shock-mitigation potential validated through the use of test coupons [2]. Lastly, the performance of newly synthesized and tested elastomer-based shock-mitigation efficient materials, integrated (as strategically placed functional layers) into a helmet/head assembly and subjected to blast loads, can be investigated computationally and/or experimentally [3,4].

Extensive research carried out by several groups [e.g. 5–7] established polyurea as a material with an unusually high potential for blast/ballistic-impact mitigation. Consequently, polyurea is frequently used as: (a) external and internal wall-sidings and foundation coating for buildings aimed at minimizing the degree of structure fragmentation and, in turn, minimizing the extent of the associated collateral damage in the case of a bomb blast; and (b) gun-fire/ballistic resistant and explosion/blast mitigating coating/liner or inter-layer in blast-resistant sandwich panels for military vehicles and structures. In our recent computational work [3,4], it was demonstrated that polyurea can also provide blast-mitigation effects when used as suspension-pad material in advanced combat helmet applications. The work presented in Refs. [3,4] clearly identified a need for a better understanding of the mechanical response of polyurea under high deformation rate, large strain high-pressure loading conditions encountered during blast loading and for a better understanding of shock-wave generation, propagation and structure as well as for the nature of energy-dissipative processes at the shock front, in this material. In the present work, an attempt is made to get a deeper insight

* Corresponding author at: 241 Engineering Innovation Building, Clemson, SC 29634-0921, United States. Tel.: +1 864 656 5639; fax: +1 864 656 4435.
E-mail addresses: mica.grujicic@ces.clemson.edu, gmica@clemson.edu (M. Grujicic).

0921-5093/$ – see front matter © 2011 Elsevier B.V. All rights reserved.
doi:10.1016/j.msea.2011.01.081

Report Documentation Page

Form Approved
OMB No. 0704-0188

1. REPORT DATE	2. REPORT TYPE	3. DATES COVERED
JAN 2011		**00-00-2011 to 00-00-2011**

4. TITLE AND SUBTITLE	5a. CONTRACT NUMBER
Molecular-level simulations of shock generation and propagation in polyurea	5b. GRANT NUMBER
	5c. PROGRAM ELEMENT NUMBER
6. AUTHOR(S)	5d. PROJECT NUMBER
	5e. TASK NUMBER
	5f. WORK UNIT NUMBER
7. PERFORMING ORGANIZATION NAME(S) AND ADDRESS(ES) **Clemson University,Department of Mechanical Engineering,241 Engineering Innovation Building,Clemson,SC,29634**	8. PERFORMING ORGANIZATION REPORT NUMBER
9. SPONSORING/MONITORING AGENCY NAME(S) AND ADDRESS(ES)	10. SPONSOR/MONITOR'S ACRONYM(S)
	11. SPONSOR/MONITOR'S REPORT NUMBER(S)

12. DISTRIBUTION/AVAILABILITY STATEMENT
Approved for public release; distribution unlimited

13. SUPPLEMENTARY NOTES

14. ABSTRACT

A non-equilibrium molecular dynamics method is employed in order to study various phenomena accompanying the generation and propagation of shock waves in polyurea (a micro-phase segregated elastomer). Several recent studies reported in the literature suggested that polyurea has a relatively high potential for mitigation of the effects associated with blast and ballistic impact. This behavior of polyurea is believed to be closely related to its micro-phase segregated microstructure (consisting of the so-called ?hard domains? and a soft matrix) and to different phenomena/processes (e.g. inelastic-deformation and energy-dissipation) taking place at, or in the vicinity of, the shock front. The findings obtained in the present analysis are used to help elucidate the molecular-level character of these phenomena/processes. In addition, the analysis yielded the shock Hugoniot (i.e. a set of axial stress vs. density/specific-volume vs. internal energy vs. particle velocity vs. temperature vs. shock speed) material states obtained in polyurea after the passage of a shock wave. The availability of a shock Hugoniot is critical for construction of a high deformation-rate, large-strain, high pressure material models which can be used within a continuumlevel computational analysis to capture the response of a polyurea-based macroscopic structure (e.g. blast-protection helmet suspension pads) to blast/ballistic impact loading.

15. SUBJECT TERMS

16. SECURITY CLASSIFICATION OF:			17. LIMITATION OF ABSTRACT	18. NUMBER OF PAGES	19a. NAME OF RESPONSIBLE PERSON
a. REPORT	b. ABSTRACT	c. THIS PAGE			
unclassified	**unclassified**	**unclassified**	**Same as Report (SAR)**	**10**	

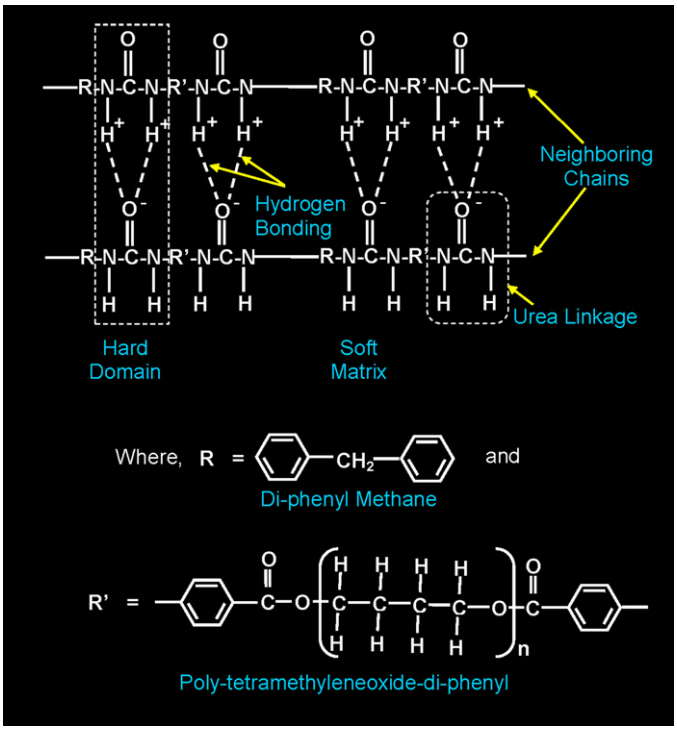

Fig. 1. A schematic of the simplified molecular-level structure of segmented polyurea.

into the various shock related phenomena in polyurea via the use of molecular-level computational analyses.

Polyurea is an elastomeric co-polymer formed by the rapid chemical reaction between an isocyanate (organic chemical containing isocyanate –N=C=O groups) and an amine (organic chemical containing amine $-NH_2$ groups). Due to the presence of strongly polar "urea linkages", polyurea is typically nano-/micro-phase segregated into the so-called "hard domains" (a high glass transition temperature, T_g, hydrogen-bonded phase) and a soft matrix (a low T_g compliant phase). Since hydrogen bonding provides inter-chain joining, polyurea is often referred to as being a thermo-plastically cross-linked (in contrast to more commonly covalently cross-linked) polymer. A schematic is provided in Fig. 1 in order to identify the basic molecular-level structural elements in polyurea.

As mentioned earlier, the main objective of the present work is to investigate various shock-wave related phenomena using molecular-level computational methods.

A shock wave (or simply a shock) is a wave which propagates through a medium at a speed higher than the sound speed and its passage causes an abrupt and discontinuous change in the material state variables (e.g., pressure, internal energy, density, temperature and particle velocity). The magnitude of the state-variable changes and the shock speed increase with the strength of the shock. While acoustic waves give rise to isentropic changes in the material state variables, passage of a shock is typically associated with irreversible (entropy-increasing) changes in the same variables. The reason behind this difference is that shock involves very high strain rates that bring energy-dissipative viscous effects into prominence.

A review of the literature carried out as a part of the present work revealed that the molecular-level computational methods were first employed to study shock waves more than 30 years ago [8–11]. While the initial studies focused on shock phenomena in dense fluids, subsequent work also included single-crystalline solids. The key findings related to the generation and propagation of shocks in these solids can be summarized as follows: (a) these phenomena are inherently more complex in solids than in fluids, because solids, in addition to the lattice parameter, introduce a new length scale (i.e. the size/spacing of defects) which tends to control the nature/extent of inelastic-deformation and dissipative processes at the shock front; (b) shock propagation typically results in the formation of steady (time-invariant) waves, and this process is facilitated by the transverse displacement of atoms which produce inelastic deformation. This deformation involves concerted slippage of atoms over each other (and not viscous flow as in the case of shocks in fluids); (c) in order to eliminate free-surface effects, molecular-level modeling of shock is typically carried out using computational systems with periodic boundary conditions (at least in directions transverse to the shock-wave propagation direction). To attain steady wave conditions of the shock, computational domains sufficiently long in the direction of shock wave propagation have to be employed. Furthermore, lateral dimensions of the computational domain have to be also sufficiently large to avoid spurious effects associated with the use of the periodic boundary conditions. Consequently, computational domains involving several tens to hundred thousands of atoms have to be employed. The corresponding computational times (controlled by the shock wave transversal time) are then on the order of 5–20 ps. This limits the shock thicknesses to around 10 nm and the corresponding rise times to ca. 0.5–1 ps. Thus, weak shock waves with thicknesses of hundreds of nanometers could not be analyzed using molecular-level methods (at least in their steady-wave regime).

While recognizing the aforementioned aspects and potential limitations of molecular-level modeling of shock, a preliminary computational study of shock generation/propagation in polyurea is carried out. There are two main objectives of the present work:

(a) To determine the shock Hugoniot (centered on the initial stress-free quiescent state) of polyurea. A Hugoniot is the locus of axial stress vs. specific volume vs. energy density (vs. particle velocity vs. shock speed) shocked ("upstream") material states. The shock Hugoniot (or simply, the Hugoniot) is often used in the derivation of the continuum-level material models (particularly in the derivation of the equation of state) which is used in the computational investigations of the response of structures to shock loading. In situations in which one is interested only in the problem of planar shock propagation/interaction (in the presence of uni-axial strain deformation states), a complete definition of the continuum-level material model is not required. Instead, the knowledge of the corresponding Hugoniot relations is sufficient; and

(b) The Hugoniot relations mentioned in (a) provide a global statement of mass, momentum, and energy conservation accompanying shock-induced material transition from a given initial ("downstream") equilibrium state to all possible final ("upstream") equilibrium states for steady planar shock waves (of different strengths). However, these relations provide no information about the structure of the shock front or the nature of the dissipative structural rearrangement mechanisms that lead to a steady shock wave. Hence, the second objective of the present work is to carry out a detailed examination of the downstream, shock-front and upstream material states (as represented by the local stresses, strains, densities/specific volumes, temperatures, etc.) and molecular-level morphology in order to identify and characterize these processes.

The organization of the paper is as follows: a brief overview of the molecular-level computational procedure including the computational cell construction, force field identification, computational method(s) selection, shock-wave generation and the problem definition are respectively presented in Sections 2.1–2.5. The key results obtained in the present work are presented and dis-

cussed in Section 3. A summary of the work carried out and the key results/conclusions are given in Section 4.

2. Molecular-level computational procedure

As mentioned earlier, molecular-level computational methods have been employed in the present work in order to investigate shock formation and propagation in polyurea. Within these methods, all atoms and bonds are explicitly accounted for and molecular mechanics, dynamics or Monte Carlo algorithms are used to quantify the behavior of the material under investigation.

While ab initio quantum mechanics methods have the advantage over the molecular-level methods since they do not require parameterization, they have a serious short-coming. Namely, due to prohibitively high computational cost, they can be currently employed only for systems containing no more than a few hundred atoms/particles. As will be shown below, while ab initio quantum-mechanics calculations are not directly used in the present work, some of the computational ab initio quantum mechanics results are used in the parameterization of the material model at the molecular length/time scale. Utility of the molecular-level computational results is greatly dependent on accuracy and fidelity of the employed force field (the mathematical expression which describe various bonding and non-bonding interaction forces between the constituents of the molecular-scale model). In the present work, the so-called "COMPASS" (Condensed-phase Optimized Molecular Potentials for Atomistic Simulation Studies) force field is used [12,13]. This highly accurate force field is of an ab initio type since most of its parameters were determined by matching the predictions made by the ab initio quantum mechanics calculations to the condensed-matter experimental data. Hence, it should be recognized that the COMPASS force field is a prime example of how the highly accurate results obtained on one length/time scale (quantum mechanic/electronic, in the present case) and the experimental data can be combined to parameterize material models used at coarser length/time scale (the molecular length/time scale, in the present case).

Formulation of a molecular-level simulation problem requires, at a minimum, specification of the following three aspects: (a) a molecular-level computational model consisting of atoms, ions, functional groups and/or molecules; (b) a set of force field functions; and (c) a computational method(s) to be used in the simulation. More details of these three aspects of the molecular-level modeling and simulations of polyurea are provided below.

2.1. Computational model

The first step in the molecular-level computational analysis was the construction of a single polyurea molecule. This was carried out using the Visualizer [14] program from Accelrys. A close-up view of a typical polyurea molecule obtained is shown in Fig. 2(a). For clarity, different atomic species and functional groups are labeled in this figure. Also, a zoomed-out view of a longer segment of the single polyurea molecule is shown as an inset in Fig. 2(a). It should be noted that the polyurea molecule analyzed in the present work is based on an isocyanate consisting of di-phenyl methane functional group and a diamine consisting of poly-tetramethyleneoxide-di-phenyl functional group (consisting of 14 C_2H_8O units), to comply with the type of polyurea being investigated experimentally in our ongoing work [2].

In order to model the behavior of bulk polyurea (i.e., in the absence of any free-surface effects) at the molecular length-scale, a rectangular box-shaped computational unit-cell is constructed and the periodic boundary conditions are applied across the faces of the cell. The three edges (a, b and c) of the cell are aligned respectively with the three coordinate axes (x, y and z). The molecular configuration within the cell containing polyurea chains whose construction was described earlier is generated using the following procedure:

(a) The molecular chain constructed above is first grown by a copy-and-attach process in order to increase its length/molecular weight;
(b) The single polyurea chain constructed in (a) is next used within the Amorphous Cell program from Accelrys [15] to fill the parallelepiped-shaped computational cell of a preselected size (7.35 nm × 1.84 nm × 1.84 nm) while attaining the target ambient-pressure density (1300 kg/m^3) of polyurea. The size of the computational cell was selected in such a way that the following conditions are satisfied: (i) In the direction of shock propagation (direction x), the computational cell size was set to a minimum value which is both larger than the shock thickness and sufficiently large to ensure the formation of a steady shock wave; and (ii) in the lateral (y and z) directions, the size of the computational cell was set to a minimal value which enables a realistic analysis of the (material) transverse flow; and
(c) The molecular configuration obtained in (b) is optimized by minimizing its potential energy with respect to the positions of the constituent atoms.

An example of the molecular-level computational-cell used in the present work is displayed in Fig. 2(b). This cell contains 1120 atoms of carbon, 1104 atoms of hydrogen, 128 atoms of nitrogen and 192 atoms of oxygen.

As discussed earlier, as-synthesized polyurea is typically micro-phase segregated and consists of hard domains and a soft matrix. In contrast, the atomic scale polyurea model as depicted in Fig. 2(b) represents a completely mixed state of this material. As discussed in our prior work [1], within the atomic scale computational methods used, micro-phase separation processes cannot be generally investigated. The main reasons for this are as follows:

(a) Within the molecular statics, local minimization algorithms are employed which are capable of only finding a minimum energy configuration of the given state of the material and typically do not involve large-scale displacement of the chain segments or chains; and
(b) Molecular dynamics is dominated by high frequency atomic vibrations and unrealizable computational times are needed to simulate phase separation using this approach.

Hence, atomic-scale calculations based on the unit cell displayed in Fig. 2(b) can only provide information about the fully mixed material state/properties, i.e., information about the material which resembles the soft-matrix phase of polyurea. It should be recalled that, within the soft matrix, hard and soft segments are well mixed and, hence, the atomic scale material model depicted in Fig. 2(b) is a fairly realistic representation of this phase of the polyurea.

To gain some insight into the molecular-level response of micro-phase segregated polyurea, a procedure is developed for rearrangement of the polyurea topology so that the average distance between the urea linkages is greatly reduced. This, in turn, resulted in a substantially larger contribution of hydrogen bonding to the non-bond potential energy of polyurea. An example of a typical local atomic arrangement in "*fully-mixed*" and the "*segregated*" polyurea is depicted in Fig. 2(c) and (d), respectively. The urea linkages can be readily identified in these figures by the presence of the blue-colored nitrogen atoms. It should be noted that although the polyurea topology displayed in Fig. 2(c) and (d) is associated with the segregation of hard and soft segments, this segregation takes place at the few-nanometer length scale. This length-scale is substantially lower than its counterpart (tens of nanometers) in the

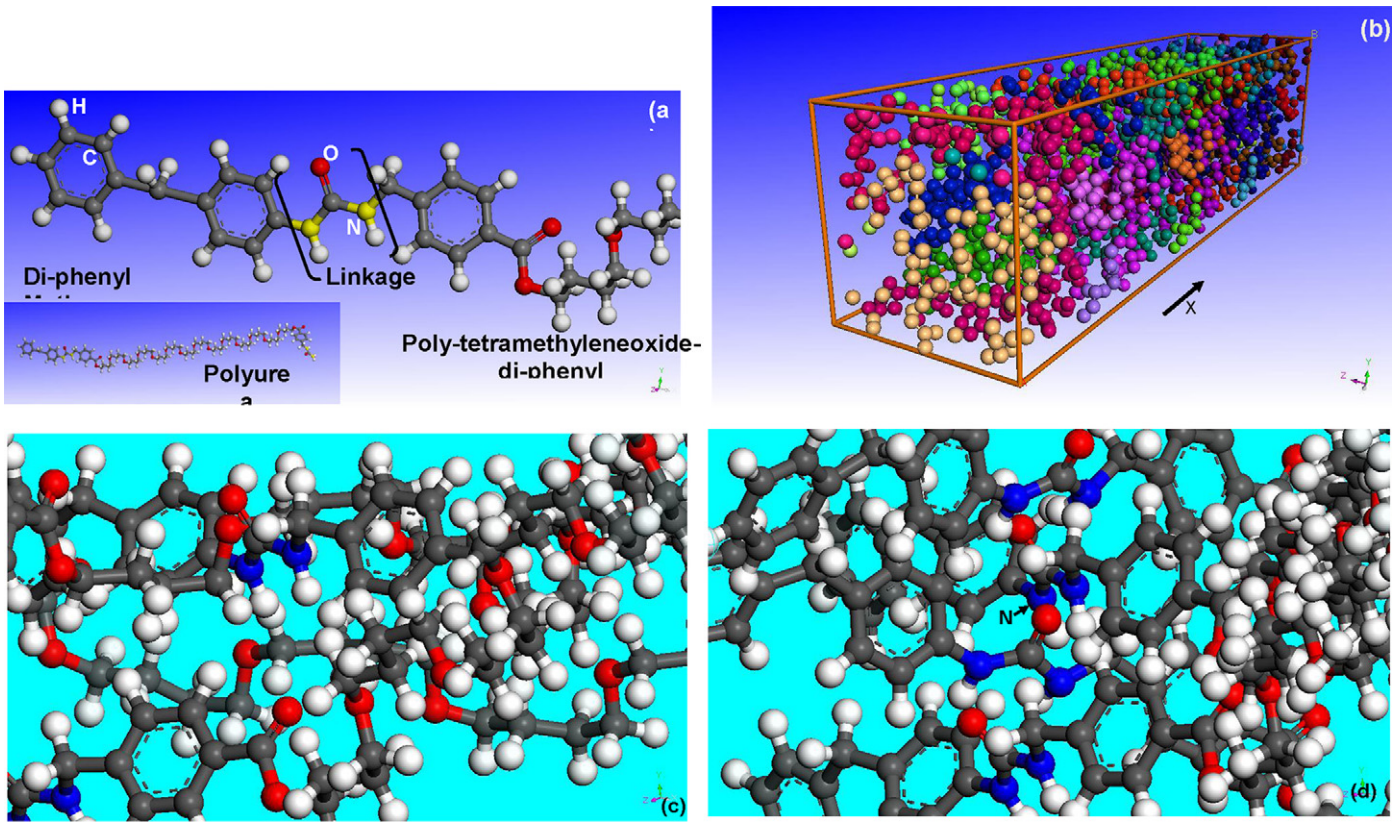

Fig. 2. (a) A segment of a single polyurea molecule with the inset showing a zoomed-out view of a longer segment of the same molecule; (b) a molecular-level computational cell in which, for clarity, each molecule is assigned a unique color; (c) and (d) local-level molecular structure in the "*fully mixed*" and "*micro-segregated*" polyurea, respectively.

case of the real polyurea. These differences are expected to affect shock-generation and propagation processes in polyurea and will be investigated in our future work.

2.2. Force-fields

As stated above, the behavior of a material system at the molecular-level is governed by the appropriate force-fields which describe, in an approximate manner, the potential energy hyper-surface on which the atomic nuclei move. In other words, the knowledge of force-fields enables determination of the potential energy of a system in a given configuration. In general, the potential energy of a system of interacting particles can be expressed as a sum of the valence (or bond), $E_{valence}$, cross-term, $E_{cross\text{-}term}$, and non-bond, $E_{non\text{-}bond}$, interaction energies as:

$$E_{total} = E_{valence} + E_{cross\text{-}term} + E_{non\text{-}bond} \quad (1)$$

The valence energy generally includes a bond stretching term, E_{bond}, a two-bond angle term, E_{angle}, a dihedral bond-torsion term, $E_{torsion}$, an inversion (or an out-of-plane interaction) term, E_{oop}, and a Urey-Bradlay term (involves interactions between two atoms bonded to a common atom), E_{UB}, as

$$E_{valence} = E_{bond} + E_{angle} + E_{torsion} + E_{oop} + E_{UB} \quad (2)$$

The cross-term interacting energy, $E_{cross\text{-}term}$, accounts for the effects such as bond length and angle changes caused by the surrounding atoms and generally includes: stretch-stretch interactions between two adjacent bonds, $E_{bond\text{-}bond}$, stretch-bend interactions between a two-bond angle and one of its bonds, $E_{bond\text{-}angle}$, bend-bend interactions between two valence angles associated with a common vertex atom, $E_{angle\text{-}angle}$, stretch-torsion interactions between a dihedral angle and one of its end bonds, $E_{end\_bond\text{-}torsion}$, stretch-torsion interactions between a dihedral angle and its middle bond, $E_{middle\_bond\text{-}torsion}$, bend-torsion interactions between a dihedral angle and one of its valence angles, $E_{angle\text{-}torsion}$, and bend-bend-torsion interactions between a dihedral angle and its two valence angles, $E_{angle\text{-}angle\text{-}torsion}$, terms as:

$$E_{cross\text{-}term} = E_{bond\text{-}bond} + E_{angle\text{-}angle} + E_{bond\text{-}angle} + E_{end\_bond\text{-}torsion} + E_{middle\_bond\text{-}torsion} + E_{angle\text{-}torsion} + E_{angle\text{-}angle\text{-}torsion} \quad (3)$$

The non-bond interaction term, $E_{non\text{-}bond}$, accounts for the interactions between non-bonded atoms and includes the van der Waals energy, E_{vdW}, and the Coulomb electrostatic energy, $E_{Coulomb}$, as:

$$E_{non\text{-}bond} = E_{vdW} + E_{Coulomb} \quad (4)$$

As mentioned earlier, the present molecular-level analysis of polyurea employs the COMPASS [12,13] force-field for various bond and non-bond interaction energies appearing in Eqs. (1)–(4). A summary of the COMPASS force-field functions can be found in our previous work [16].

2.3. Computational method

Both molecular statics and molecular dynamics simulations were employed in the present work. Within the molecular statics approach, the unit-cell potential energy (as defined by Eqs. (1)–(4)) is minimized with respect to the position of the constituent particles/atoms. The potential energy minimization within Discover [17] (the atomic simulation program from Accelrys used in the present work) is carried out by combining the Steepest Descent, Conjugate Gradient and the Newton's minimization algorithms. These algorithms are automatically inactivated/activated as the atomic configuration is approaching its energy minimum (i.e. the Steepest

Descent method is activated at the beginning of the energy minimization procedure while the Newtons' method is utilized in the final stages of this procedure).

As will be discussed in greater detail in Section 3, molecular statics is employed to determine the state of the material swept by a shock. As will be shown, this procedure is based on the use of (bonding and non-bonding) potential energy components and neglects shock-induced changes in the (configurational) entropy of the system. To assess the consequence of this simplification, the approach described in Ref. [18] was considered. This approach defines a dimensionless parameter and states that when this parameter is significantly smaller than unity, entropy effects can be neglected. Unfortunately, detailed temperature and pressure dependencies of the material mechanical response of polyurea needed to evaluate this parameter were not available with sufficient fidelity. Hence, the results obtained by the application of this procedure, which suggest that the entropy effects may not be highly critical, cannot be accepted with a high level of confidence.

Within the molecular dynamics approach, gradient of the potential energy with respect to the particle positions is first used to generate forces acting on the particles and, then, the associated Newton's equations of motion (for all particles) are integrated numerically in order to track the temporal evolution of the particle positions. Both the equilibrium and non-equilibrium molecular dynamics methods are employed in the present work. Within the equilibrium molecular-dynamics methods, the system under consideration is coupled to an (external) environment (e.g. constant pressure piston, constant temperature reservoir, etc.) which ensures that the system remains in equilibrium (i.e. the system is not subjected to any thermodynamic fluxes). As will be discussed in next section, *NVT* (where N is the (fixed) number of atoms, V, the computational cell volume (also fixed), and $T = (298\,\mathrm{K})$ is the temperature) equilibrium molecular dynamics is employed in the first stage of the shock generation procedure. In addition, as will be discussed in Section 3, *NVE* (E is the total energy) equilibrium molecular dynamics is also employed during determination of the shock Hugoniot. Within non-equilibrium molecular dynamics, the system is subjected to large perturbations (finite changes in the axial parameter of the computational cell, in the present case) which create a thermodynamic flux (i.e. the flux of energy and momentum, in the present case). More details regarding the use of Discover to carry out molecular statics and molecular dynamics analyses can be found in our prior work [1].

2.4. Shock-wave generation

To generate a planar shock (or more precisely a pair of planar shocks) within the computational cell, the following procedure is employed:

(a) At the beginning of the analysis, a "sufficiently long" NVT molecular dynamics simulation is carried out in order to equilibrate the system/material.
(b) The shock is then initiated (and driven) by continuously contracting the computational cell x-direction lattice parameter a as:

$$a(t) = a(t = 0) - 2u_p t \tag{5}$$

where t denotes time, u_p is the so-called "piston" velocity (or equivalently the particles upstream velocity) in the x-direction. u_p is varied over a range between 187.5 and 1500 m/s in order to simulate the generation and propagation of shock of various strengths. Meanwhile, computational-cell transverse lattice parameters b and c are kept constant in order to obtain planar (uniaxial-strain) shock conditions. In this process, the computational cell faces normal to the shock propagation-direction behave very similarly to the impact-surface of a plate-like target subjected to a so-called symmetric "flyer-plate" impact test [19]. The procedure employed here generates a pair of shock waves which propagate, at a shock speed U_s, from the cell boundaries towards its center. As schematically shown in Fig. 3, these shock waves leave behind a "shocked" material state characterized by a higher material mass density (as well as by higher levels of the internal energy, stress, particle velocity, temperature and entropy).

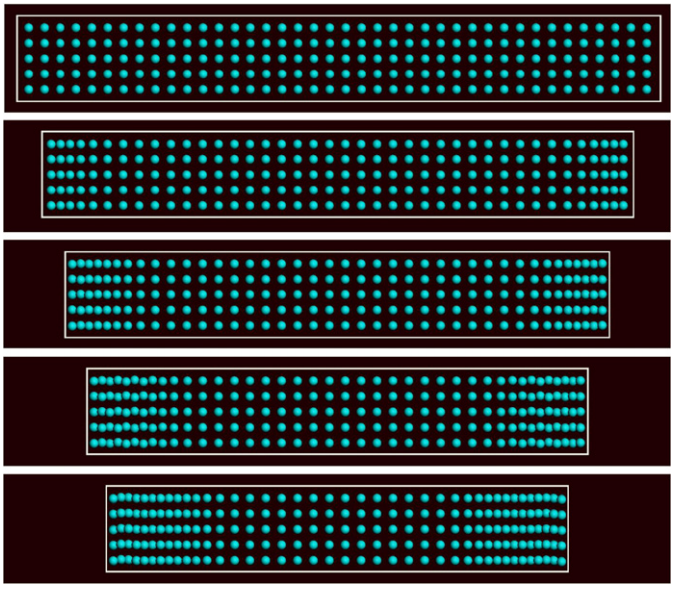

Fig. 3. A schematic of the generation of a pair of shocks in a molecular-level system via the process of computational-cell parameter contraction.

The aforementioned procedure for shock-wave generation and the subsequent molecular statics/dynamics analyses are carried out through the use of a Discover input file [17] which is written in a BTCL (Basic Tool Command Language) language. This enabled the use of a scripting engine that provides very precise control of simulation jobs, e.g. a cell deformation to be carried out in small steps each followed by a combined energy-minimization/molecular-dynamics simulation run.

2.5. Problem formulation

The problem addressed in the present work involved generation of shock waves of different strengths (using the aforementioned computational cell parameter contraction method), determination of the associated shock-Hugoniot relations and identification and elucidation of the main molecular-level inelastic-deformation/energy dissipation processes taking place at or in the vicinity of the shock front. The procedure for shock wave generation was presented in the previous section.

As far as the shock Hugoniot determination is concerned, it entailed the knowledge of the shock-wave profiles (and their temporal evolution) for the axial stress, material density, particle velocity, internal energy and temperature. The latter are obtained by lumping particles/atoms and their (bond and non-bond) potential and kinetic energy contributions into fixed-width bins, in the order of their axial coordinates. As will be shown in the next section, two types of bins are used: (a) a Lagrangian-type which is fixed to the initial/reference state of the computational cell and (b) a moving-type which is attached to the advancing shock front.

Identification of the molecular-level inelastic-deformation/energy dissipation processes entailed a close

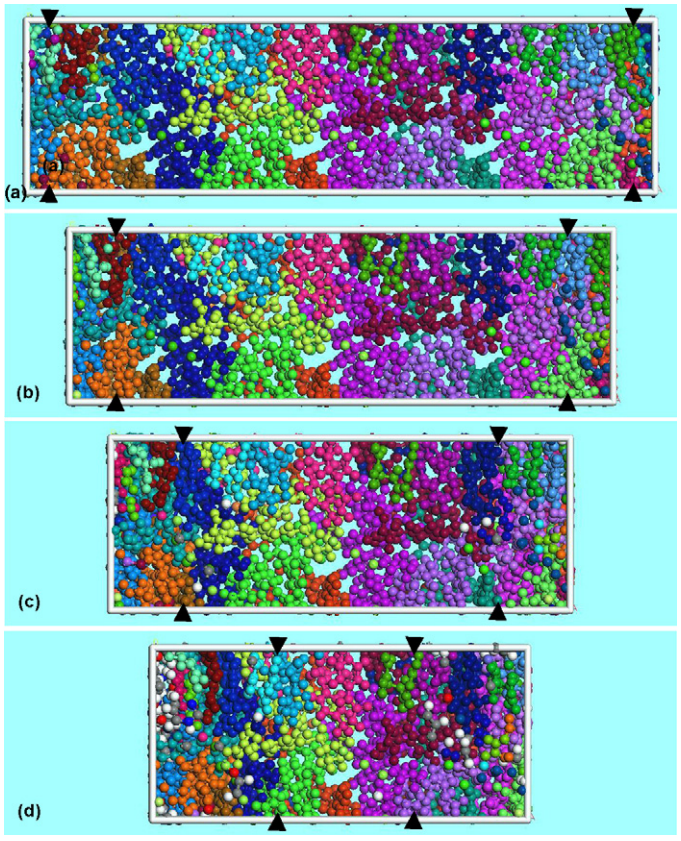

Fig. 4. Temporal evolution of the molecular level material microstructure accompanying generation and propagation of a pair of planar shocks.

examination of the changes in a material bond structure and topology caused by the passage of the shock.

3. Results and discussion

3.1. Shock-wave observation and structure characterization

An example of the typical results, obtained in the present work, pertaining to material molecular-level microstructure/topology evolution caused by a continuous axial contraction of the computational cell is displayed in Fig. 4(a)–(d). The results displayed in these figures clearly reveal the generation of a pair of planar shock waves at the two y–z faces of the computational cell, Fig. 4(a), and their subsequent propagation towards the center of the cell, Fig. 4(b)–(d). An approximate location of the center-point of the two shocks is indicated using arrowheads in Fig. 4(a)–(d). While the two shocks collide at a later simulation time, a shock-wave interaction investigation is beyond the scope of the present work. The results displayed in Fig. 4(a)–(d) show that the shock waves remain fairly planar during their motion.

While the results displayed in Fig. 4(a)–(d) provide clear evidence for the formation and propagation of a pair of opposing planar shock waves, they do not offer any information about the structure/shape of the shock-wave front or about the state of the (upstream) material swept by the shock. The latter aspects of shock-wave generation and propagation within polyurea are addressed in the remainder of this section and in the subsequent sections.

To reveal the structure/shape of the shock wave, the method of (Lagrangian) bins described in Section 2.4 is employed. In this case, the bins are fixed in the (initial) reference configuration of the computational cell. In other words, the same atoms are associated with a given bin throughout the entire molecular dynamics simulation.

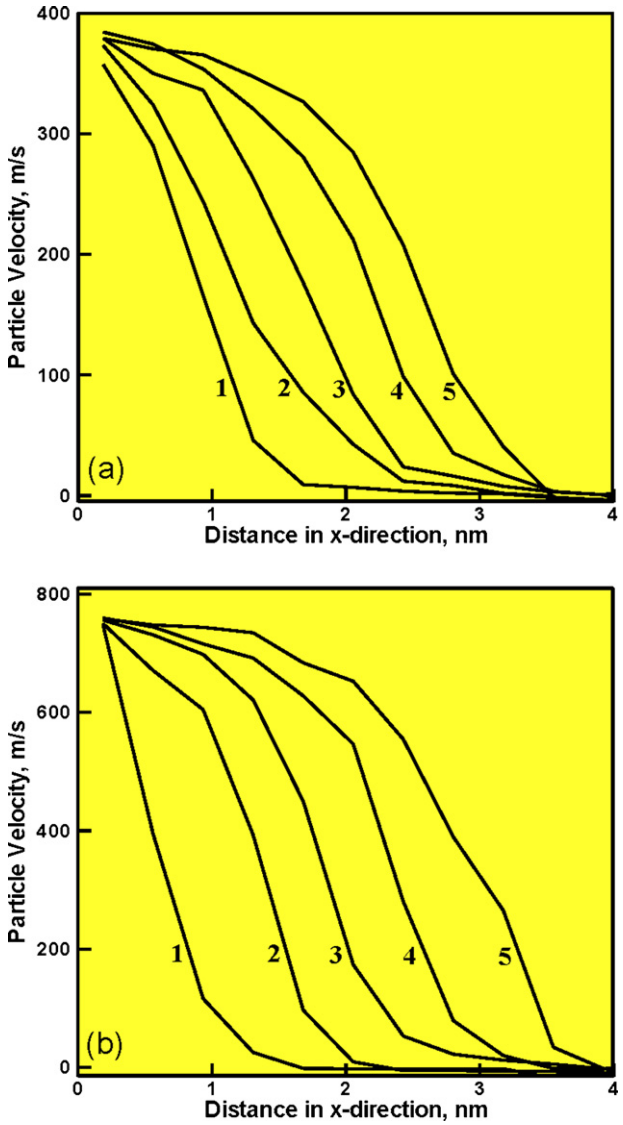

Fig. 5. (a) Temporal evolution of the particle velocity associated with the propagation of two approaching shock waves. The results in (b) are associated with a 50% higher computational-cell axial contraction rate.

Examples of the typical results obtained through the use of this method are displayed in Fig. 5(a) and (b). The results displayed in Fig. 5(a) and (b) are obtained under identical conditions except for the rate of axial contraction of the computational cell (50% higher in the case of Fig. 5(b)). In these figures, particle velocities at different simulation (i.e. post shock wave generation) times are plotted against the Lagrangian bin center x-location. Brief examination of the results displayed in these figures reveals that:

(a) two shock waves are generated (only the right-propagating shock is shown though) at the computational cell faces normal to the x-direction. These shocks then propagate towards the computational-cell center;
(b) after a brief transient period, the shocks appear to reach a steady wave profile (i.e. a time-invariant profile within a reference frame which is attached to, and moves with, the shock front); and
(c) both the particle velocity and the shock speed increase with the computational-cell contraction rate. It should be noted that the curves bearing the same numerical label in Fig. 5(a) and (b) correspond to the same simulation time.

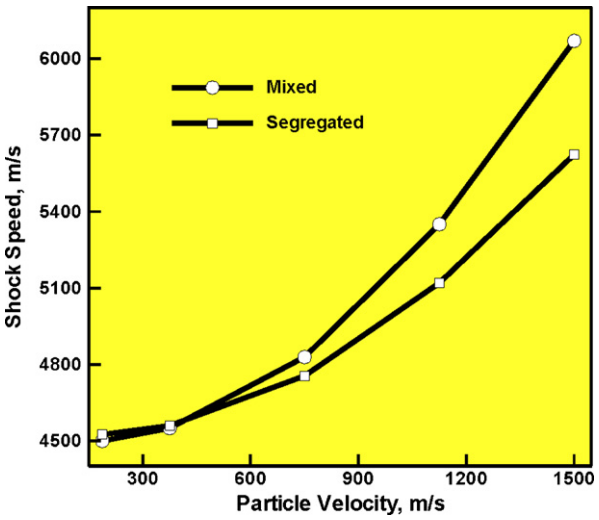

Fig. 6. The Hugoniot relation pertaining to the particle velocity dependence of the shock speed.

It should also be noted that no thermostat was used in the present non-equilibrium molecular dynamics simulations, so that the steady-wave shock profile is a natural consequence of a balance between the continuous supply of momentum to the system (through the continuous computational cell axial contraction) and the observed lateral motion of the atoms in the continuously enlarged upstream material domain swept by the shock. In general, the use of a thermostat modifies the ($F=ma$ Newtonian-type) equations of motion solved within the molecular dynamics simulations by the introduction of a (velocity-proportional) viscous-dissipation term. It is well-established that, when shock formation and propagation is analyzed within a continuum framework, the use of a viscous-dissipation term is mandatory for the attainment of a steady-wave shock profile. This fact has often been used as a justification for the use of a (local or global) thermostat within molecular-level simulations of shock-wave formation/propagation. While such practices greatly facilitate the attainment of a steady shock, they cannot be readily defended since shock formation and propagation is generally considered to be an adiabatic (no system/surrounding energy exchange) process due to the near-instantaneous material transition to the shocked state. In addition, shock generation/propagation is a non-isentropic process due to the attendance of various energy dissipation mechanisms. This is the main reason that no thermostat was used in the present work. It is interesting to point out that despite the fact that no viscous-dissipation term was added to the Newton's equations of motion, the results displayed in Fig. 5(a) and (b) show some of the defining features of shock-waves when they are analyzed in the continuum-level simulations (in the presence of viscous dissipation). Specifically, a steady shock is generated and the shock width decreases with an increase in the shock strength.

3.2. Determination of shock-Hugoniot relations

The results presented in Fig. 5(a) and (b) reveal the steady-shock profile and can be used to find a functional relation between the shock speed, U_s, and the particle velocity, u_p. This was done in the present work and the results obtained are displayed in Fig. 6. The two curves displayed in Fig. 6 labeled respectively as "mixed" and "segregated" correspond to the fully mixed and micro-phase segregated initial states of the polyurea. The U_s vs. u_p relation is one of the so-called shock Hugoniot relations. In general, the Hugoniot can be defined as a locus of shocked-material states in a stress/pressure, energy density, mass density (or specific volume), temperature, particle velocity and shock speed space which are associated with (or "centered at") a given initial/reference material state. The U_s vs. u_p relation mentioned above is a simple projection of the Hugoniot to the U_s–u_p plane. In the case of planar shocks, of interest in the present work, the other commonly used Hugoniot relations include: axial stress, t_{11}, vs. density, ρ (or specific volume, $v = 1/\rho$); (mass-based) internal energy density, e, vs. ρ (or v); t_{11} vs. u_p and temperature T vs. ρ (or v). These relations were determined in the present work using two distinct methods:

(a) The first method is based on the three so-called "jump equations" which are defined as:

$$\rho^- U_s = \rho^+ (U_s - u_p) \tag{6}$$

$$t_{11}^- + \rho^- U_s^2 = t_{11}^+ + \rho^+ (U_s - u_p)^2 \tag{7}$$

$$e^- + \frac{t_{11}^-}{\rho^-} + 0.5 U_s^2 = e^+ + \frac{t_{11}^+}{\rho^+} + 0.5 (U_s - u_p)^2 \tag{8}$$

These equations relate the known downstream material states (denoted by a superscript "−") and the unknown upstream material states (denoted by a superscript "+") associated with the shock of a given strength (as quantified by the shock speed or the downstream-to-upstream particle velocity jump). These equations are next combined with the previously determined U_s vs. u_p relation and the prescribed (shock-strength defining quantity) U_s or u_p to solve for the unknown upstream material states. It should be noted that this method enables determination of only material mechanical state variables (t_{11}, e, $v(=1/\rho)$, U_s and u_p). To obtain temperature, a separate set of equilibrium *NVE* (E-total energy of the system) molecular dynamics simulations is carried out. In each case, a local computational sub-cell is defined containing only the upstream (shocked) material. The number of particles, the volume of the sub-cell and its total internal energy are all maintained constant. The associated "*equilibrium*" temperature is then calculated using the time-averages of the atomic velocities (see Eq. (10) below); and

(b) Time averages of the atomic positions, r_i, velocities, v_i, and interaction forces, f_i (i is the atomic label) are used to compute the unknown, local (bin-based) thermo-mechanical quantities using the following standard thermodynamic relations:

$$\rho = \frac{1}{V_{bin}} \left[\left(\sum_{i=1}^{N_{bin}} m_i \right)_{avg} \right] \tag{9}$$

$$T = \left(\frac{1}{3 N_{bin} k_b} \left[\sum_{i=1}^{N_{bin}} m_i v_i . v_i \right] \right)_{avg} \tag{10}$$

$$t_{11} = \frac{1}{V_{bin}} \left(N_{bin} k_b T + \sum_{i=1}^{N_{bin}} r_i \otimes f_i \right)_{avg} \tag{11}$$

$$E = \left(E_{Total} + \frac{1}{2} \left(\sum_{i=1}^{N_{bin}} m_i v_i . v_i \right) \right)_{avg} \tag{12}$$

where subscript "avg" denotes time averaging, N_{bin} and V_{bin} the number of atoms within and the volume of the bin, respectively, k_b is the Boltzmann's constant, E_{Total} is given by Eq. (1), while "·" and "⊗" indicate dot product and tensorial product operators, respectively.

It should be noted that, in this case, the bins were defined within a reference frame which is attached to (and moves with)

the steady-shock front. Clearly, in this case different atoms may reside within a given bin at different simulation times. On the other hand, the bins correctly collect the information about the atoms (temporarily) residing in a given portion of the steady-shock profile. In other words, time averages are calculated not for a fixed assembly of atoms, but rather for a transient set of atoms associated with a given moving bin. It should be also noted that since one of the main objectives of the present work was determination of the Hugoniot relations, only the data pertaining to the bins located in the upstream portion of the shock-wave are collected and analyzed (for different shock-strength conditions).

The results of these two procedures are displayed in Fig. 7(a)–(d). In each of these figures, two cases are shown and labeled as "*Method (a)*" or "*Method (b)*" in order to indicate the method used for generation of the corresponding results. In addition, separate curves are given for the two initial conditions of polyurea. It is apparent that the two methods yield consistent results while the initial ("*mixed*" or "*segregated*") condition of the polyurea has a noticeable effect on to the computed shock Hugoniot relations. An explanation for the latter observation will be provided in the next section.

The Hugoniot relations displayed in Figs. 6 and 7(a)–(d) are typically used within a continuum-level computational analyses of shock-wave generation/propagation in two ways:

(a) They are directly used in the analyses of shock-wave propagation under uniaxial strain conditions [e.g. 3]; and
(b) Alternatively, they can be used to derive a continuum-level material model which is consistent with the material mechanical response under high-rate, large-strain, high-pressure conditions. Such a model is subsequently used in general three-dimensional, non-linear dynamics computational analyses [4].

In our recent work [20], it was shown that the Hugoniot relations can be generated by converting the corresponding isotherms (obtained via quasi-static, molecular-level mechanical tests). This procedure was found to be associated with a number of challenges (e.g. a particular form of the equation of state had to be assumed, several material properties/relations had to be assessed independently, etc.). Most of these challenges were not encountered in the present work since the Hugoniot relations are derived more directly from the molecular-level computational results.

3.3. Shock-induced material-state changes

The results presented and discussed in the previous sections clearly revealed the formation and propagation of planar shocks in polyurea and enabled formulation of the appropriate shock-Hugoniot relations. In addition, a clear difference in the shock-wave form and the associated Hugoniot relations was observed in the cases of fully-mixed and micro-phase segregated polyurea. In the present section, a more detailed investigation is carried out of the molecular-level material microstructure in the wake of a propagating planar shock in order to provide some justification for the observed differences in a shock-wave behavior in the two polyurea initial states.

It should be first realized that the analysis of material microstructure and its evolution due to shock loading in polyurea is quite challenging due to the absence of a crystal structure in this material. Namely, when molecular-level simulations of shock generation/propagation are carried out in (nearly perfect) single crystal solids (e.g. [8,11]), deviations from long range order (i.e. formation of various point, line and planar defects) can be readily investigated. Polyurea is, on the other hand, an amorphous material in its initial condition and remains so after being subjected to the shock loading. To address the challenge of material microstructure characterization and its changes resulting from shock loading, two microstructural parameters are monitored in the present work: (a) the extent of lateral motion of the atoms at the shock front; and (b) the extent of hydrogen-bond breaking (in the case of micro-phase segregated polyurea, only).

In the case of single-crystalline solids, previous molecular-level shock-wave formation/calculation work (e.g. [8,11]) established that the steady-wave condition is attained not as a result of viscous dissipation (as is the case for shocks in fluids) but rather as a result of transverse atomic motions which result in inelastic deformation (permanent slippage of crystal planes and the formation of crystal defects). Similar lateral motion of the atoms at, or in the vicinity of, the shock front is also observed in the present work. Since these motions resulted in a permanent change in atomic nearest neighbor coordination, they can be considered as in-elastic strain producing. However, as stated earlier, the amorphous nature of polyurea precludes a more detailed/quantitative description of the nature of the atomic lateral motion process or the associated defect formation. What is certain, however, is that no covalent bond-breaking was observed to take place. In addition, shock-loading is found to lead to a permanent (1–2%) densification of this material (for both the fully-mixed and micro-phase segregated initial conditions). This finding is somewhat puzzling since polyurea, within the continuum framework, is considered as a nearly incompressible material.

Significant lateral atomic motions are observed in both the fully mixed and micro-phase segregated states of polyurea. No statistically significant differences in the extents of this motion could be detected for the two states of polyurea. However, numerous observations of hydrogen-bond breaking between urea linkages of the adjacent chains are made in the case of the micro-phase segregated polyurea. Since hydrogen-bond breaking is a fairly potent shock-wave energy absorbing/dissipating mechanism, one may expect that this process contributes significantly to the experimentally observed high blast/ballistic impact mitigation potential of polyurea.

To demonstrate that hydrogen-bond breaking leads to irreversible changes in the material properties, molecular statics-based local simple-shear tests of the upstream material were carried out. Within these tests, a local (upstream) computational cell is subjected to a sequence of simple-shear deformation modes and, in each case, an energy minimization procedure is employed. Then, the procedure used in our previous work [21–24], which relates the (minimum) energy to the first and second invariants of the left Cauchy deformation tensor, is employed in order to determine the evolution of the stress state. The initial rate of change of the resulting shear stress with the change in the shear strain is used as a measure of the material shear modulus. This procedure clearly revealed that hydrogen-bond breaking due to material exposure to shock loading leads to a 10–15% reduction in the material shear modulus. An example of the relaxed molecular-level microstructure of micro-phase segregated and shocked polyurea after being subjected to simple shear is displayed in Fig. 8.

3.4. Molecular-level impulse test

To help reveal differences in the mechanical response of fully mixed and micro-phase segregated polyurea to shock loading, a molecular-level impulse (computational) test is carried out. Within this test, the computational-cell axial lattice parameter is perturbed only once by a finite amount. This created a pair of impulse waves (one at each y–z face of the cell). The impulse essentially consists of a shock-wave closely followed by a release wave. An example of the typical results obtained in this portion of the work is given in Fig. 9 in which impulse profiles at different simulation times are shown

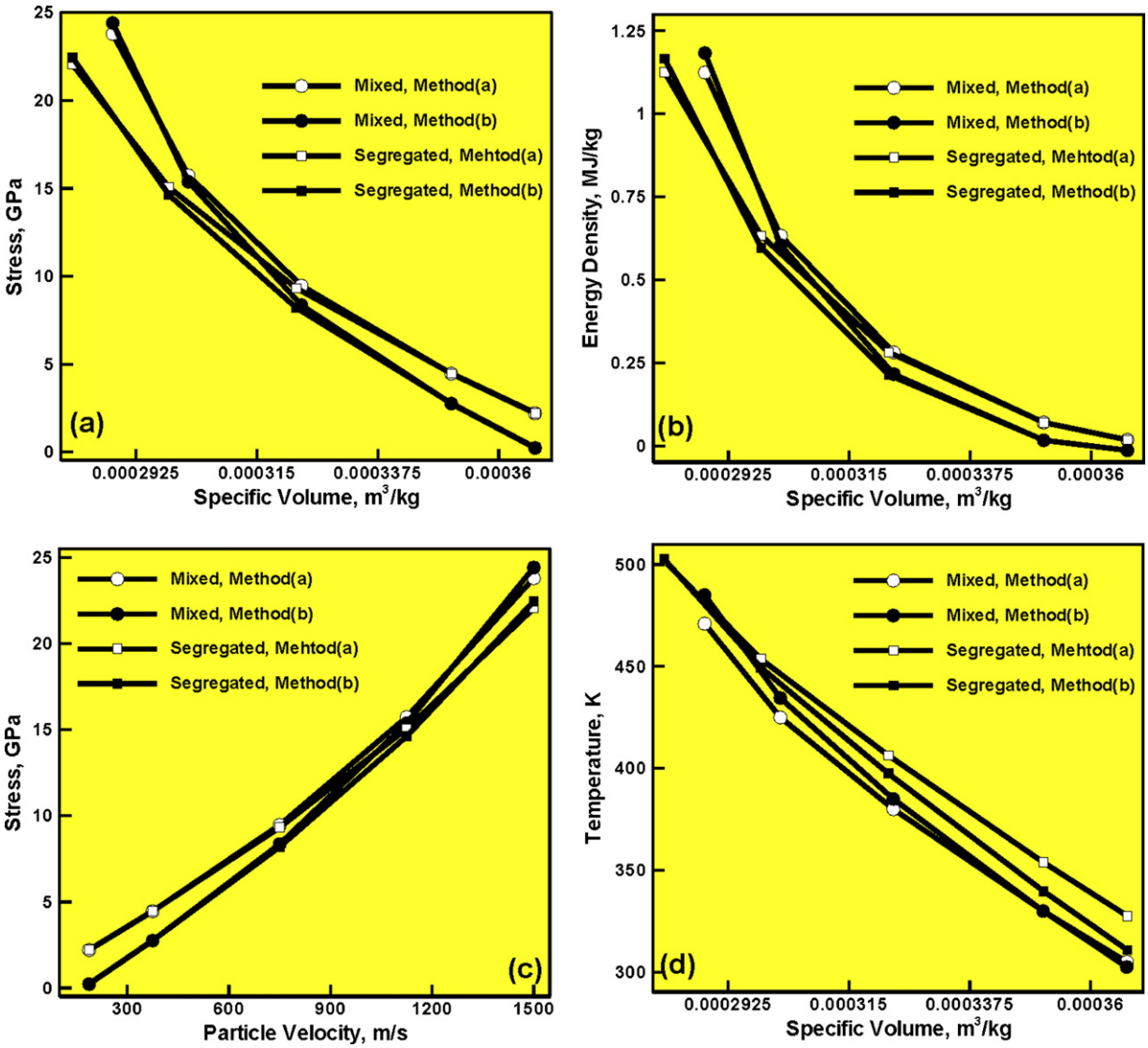

Fig. 7. (a) Axial stress vs. specific volume; (b) energy vs. specific volume; (c) axial stress vs. particle velocity; and (d) temperature vs. specific volume Hugoniot relations. Please see text for explanation of the "Method (a)" and "Method (b)".

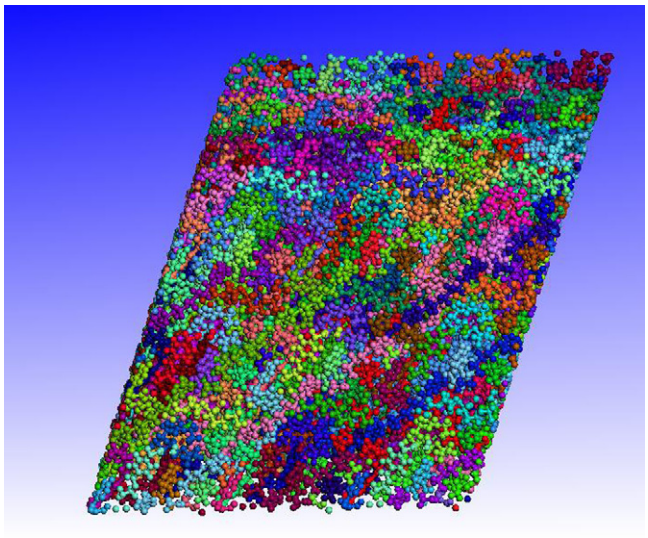

Fig. 8. Relaxed atomic configurations of the micro-phase segregated and shocked polyurea after being subjected to simple shear.

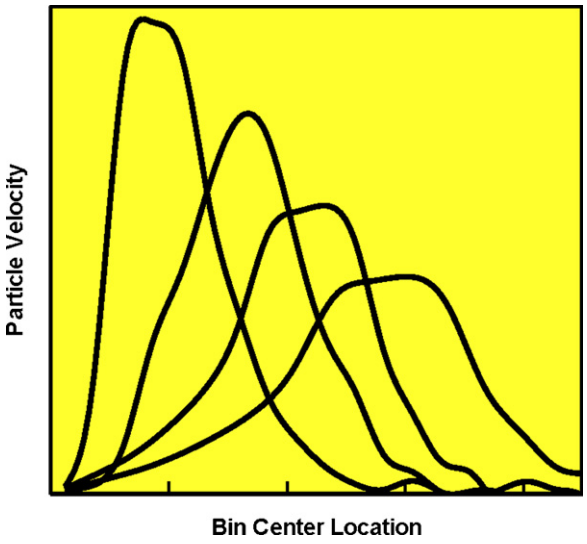

Fig. 9. An example of the typical results obtained in the present work pertaining to the temporal evolution (dispersion) of an impulse travelling to the right.

for the right-travelling impulse, only. As is seen in Fig. 9, the impulse tends to become dispersed as it advances towards the center of the computational cell. Ultimately, the impulse becomes completely dispersed (i.e. difficult to resolve). The main task within the present section was to determine if there is a statistical difference in the distance of propagation of the impulses in the two polyurea cases before the impulses become completely dispersed.

The results obtained in the present work revealed that the micro-phase segregated polyurea consistently yields a shorter impulse "*complete-dispersion*" distance (by 5–10% depending on the shock strength). While this finding is quite preliminary and requires further in depth investigation, it provides a tentative proof that shock-induced hydrogen-bond breaking plays an important role in the superior shock-impact mitigation capacity of this material.

3.5. Final remarks

Within the present work, molecular-level computational methods are employed to study various phenomena accompanying shock-wave generation and propagation in polyurea. It should be noted that the present work does not suggest that molecular-level analyses of shock generation and propagation should replace the corresponding continuum (hydrodynamic) analyses. The latter are far better suited (and feasible) for studying the behavior of real-life engineering systems (e.g. suspension layers within the blast-protection helmets). Rather, the present approach is highly beneficial relative to the identification and characterization of the nano-scale phenomena/processes taking place at the shock front. Once these phenomena/processes are well understood and characterized (a formidable task), the knowledge gained can be used to formulate (and parameterize) more physically based material models suitable for use in continuum-level analyses.

Another important aspect of the present work, worth discussing, is the size of the computational cell used. This size corresponds to the maximum size that can be handled (within realistic computational times) with the given combination of the number of software (Discover) licenses and the computer resources available during the present work. The main consequence of the relatively small computational cell used is that the present study was limited to the intermediate- and high-strength shock regimes (i.e. the regimes which are associated with a reasonably small shock width). These regimes may not be of main interest within the context of traumatic brain injury since they would (most likely) cause soldier fatality. Weaker shocks, which are not too strong to cause a soldier's death yet strong enough to cause TBI, are of major concern. These shocks are associated with a much larger width which could not be accommodated with the present size of the computational cell. We are in the process of acquiring computational capabilities which will allow us to address the weak shock-wave regime in the future. This will allow us to generate the appropriate Hugoniots and identify the nature of the energy dissipation processes in this shock-wave regime.

4. Summary and conclusions

Based on the results obtained in the present work, the following summary remarks and main conclusions can be drawn:

Various phenomena accompanying the formation and propagation of a planar shock-wave within polyurea, a micro-phase segregated elastomer, are investigated using molecular-level computational methods.

The results obtained show that even without the use of a viscous-dissipation-based thermostat, a steady-wave planar shock profile can readily be established in this material.

The time-averaged results pertaining to the atomic positions, velocities and interaction forces are used to construct the appropriate shock Hugoniot relations, the relations which define the locus of stress, energy, density, temperature and particle velocity of the material swept by a shock propagating at a given speed.

Detailed examination of the molecular-level microstructure evolution in the shock-wave wake is carried out in order to identify the nature of energy absorbing and shock-wave spreading mechanisms. The results revealed that shock loading causes extensive hydrogen bond breaking in the micro-phase segregated polyurea. These processes are associated with substantial energy absorption and dissipation and are believed to be related to the experimentally observed high blast/ballistic impact mitigation potential of polyurea.

Acknowledgements

The material presented in this paper is based on work supported by the Office of Naval Research (ONR) research contract entitled "*Elastomeric Polymer-By-Design to Protect the Warfighter Against Traumatic Brain Injury by Diverting the Blast Induced Shock Waves from the Head*", Contract Number 4036-CU-ONR-1125 as funded through the Pennsylvania State University, the Army Research Office (ARO) research contract entitled "*Multi-length Scale Material Model Development for Armor-grade Composites*", Contract Number W911NF-09-1-0513, and the Army Research Laboratory (ARL) research contract entitled "*Computational Analysis and Modeling of Various Phenomena Accompanying Detonation Explosives Shallow-Buried in Soil*" Contract Number W911NF-06-2-0042. The authors are indebted to Drs. Roshdy Barsoum of ONR and Bruce LaMattina of ARO for their continuing support and interest in the present work. The authors also want to thank professors J. Runt, J. Tarter, G. Settles, G. Dillon and M. Hargether for stimulating discussions and friendship.

References

[1] M. Grujicic, B. Pandurangan, A.E. King, J. Runt, J. Tarter, G. Dillon, Journal of Materials Science 46 (2010) 1767–1779.
[2] J. Runt, Pennsylvania State University, in preparation.
[3] M. Grujicic, W.C. Bell, B. Pandurangan, T. He, Materials and Design 31 (9) (2010) 4050–4065.
[4] M. Grujicic, W.C. Bell, B. Pandurangan, P.S. Glomski, Journal of Materials Engineering and Performance (2010), doi:10.1007/s11665-010-9724-z.
[5] M.R. Amini, A.V. Amirkhizi, S. Namet-Naser, International Journal of Impact Engineering 37 (2010) 90–102.
[6] Y.A. Bahei-El-Din, G.J. Dvorak, O.J. Fredricksen, International Journal of Solids and Structures 43 (2006) 7644–7658.
[7] R.B. Bogoslovov, C.M. Roland, R.M. Gamache, Applied Physics Letters 90 (2007) 221910.
[8] B.L. Holian, G.K. Straub, Physical Review Letters 43 (1979) 1598.
[9] G.K. Straub, S.K. Schiferl, D.C. Wallace, Physical Review B 28 (1983) 312–316.
[10] V.Y. Klimenko, A.N. Dremin, in: O.N. Breusov, et al. (Eds.), Detonatsiya, Chernogolovka, AkademiiNauk, Moscow, 1978, p. 79.
[11] B.L. Holian, W.G. Hoover, B. Moran, G.K. Straub, Physical Review A 22 (1980) 2498.
[12] H. Sun, Journal of Physical Chemistry B 102 (1998) 7338.
[13] H. Sun, P. Ren, J.R. Fried, Computational and Theoretical Polymer Science 8 (1/2) (1998) 229.
[14] http://www.accelrys.com/mstudio/ms modeling/visualiser.html.
[15] http://www.accelrys.com/mstudio/ms modeling/amorphouscell.html.
[16] M. Grujicic, Y.P. Sun, K.L. Koudela, Applied Surface Science 253 (2007) 3009.
[17] http://www.accelrys.com/mstudio/ms modeling/discover.html.
[18] D.N. Theodorou, U.W. Suter, Macromolecules 19 (1986) 139–154.
[19] A.V. Amirkhizi, J. Isaacs, J. McGee, S. Namet-Nasser, Philosophical Magazine 86 (36) (2006) 5847–5866.
[20] M. Grujicic, W.C. Bell, P.S. Glomski, B. Pandurangan, B.A. Cheeseman, C. Fountzoulas, P. Patel, D.W. Templeton, K.D. Bishnoi, Journal of Materials Engineering and Performance (2010), doi:10.1007/s11665-010-9774-2.
[21] M. Grujicic, B. Pandurangan, C.D. Angstadt, K.L. Koudela, B.A. Cheeseman, Journal of Material Science 42 (2007) 5347–5349.
[22] M. Grujicic, B. Pandurangan, T. He, B.A. Cheeseman, C.-F. Yen, C.L. Randow, Materials Science and Engineering A 527 (29–30) (2010) 7741–7751.
[23] M. Grujicic, T. He, B. Pandurangan, J. Runt, J. Tarter, G. Dillon, Journal of Materials: Design and Applications, (2011), in press.
[24] M. Grujicic, T. He, B. Pandurangan, Journal of Materials Engineering Performance, submitted for publication.